Acc. Chem. Res. **2003,** *36,* 317−326

The Mechanism of Methanol to Hydrocarbon Catalysis

JAMES F. HAW,* WEIGUO SONG,
DAVID M. MARCUS, AND JOHN B. NICHOLAS

Loker Hydrocarbon Research Institute and Department of Chemistry, University of Southern California, University Park, Los Angeles, California 90089-1661

Received October 25, 2002

ABSTRACT

The process of converting methanol to hydrocarbons on the aluminosilicate zeolite HZSM-5 was originally developed as a route from natural gas to synthetic gasoline. Using other microporous catalysts that are selective for light olefins, methanol-to-olefin (MTO) catalysis may soon become central to the conversion of natural gas to polyolefins. The mechanism of methanol conversion proved to be an intellectually challenging problem; 25 years of fundamental study produced at least 20 distinct mechanisms, but most did not account for either the primary products or a kinetic induction period. Recent experimental and theoretical work has firmly established that methanol and dimethyl ether react on cyclic organic species contained in the cages or channels of the inorganic host. These organic reaction centers act as scaffolds for the assembly of light olefins so as to avoid the high high-energy intermediates required by all “direct” mechanisms. The rate of formation of the initial reaction centers, and hence the duration of the kinetic induction period, can be governed by impurity species. Secondary reactions of primary olefin products strongly reflect the topology and acid strength of the microporous catalyst. Reaction centers form continuously through some secondary pathways, and they age into polycyclic aromatic hydrocarbons, eventually deactivating the catalyst. It proves useful to consider each cage (or channel) with its included organic and inorganic species as a supramolecule that can react to form various species. This view allows us to identify structure−activity and structure selectivity relationships and to modify the catalyst with degrees of freedom that are more reminiscent of homogeneous catalysis than heterogeneous catalysis.

Introduction

One of the most promising routes from methane to more useful chemicals began with an accidental discovery. In the early 1970s, Clarence Chang and Tony Silvestri of Mobil Central Research were trying to discover new ways to make high-octane gasoline from methanol and isobutane using Mobil’s new catalyst, an acidic aluminosilicate zeolite called HZSM-5. The Mobil workers imagined that methanol would be activated on the catalyst−possibly to either the methyl cation (CH_3^+) or carbene ($:CH_2$), and the highly reactive intermediate would then add to the alkane. Instead they observed some gaseous products and a liquid mixture of alkanes and aromatics similar to high-octane gasoline. Mass balance showed that none of the isobutane was consumed, and the same products were obtained using methanol alone. The discovery of methanol to hydrocarbon catalysis was patented in 1975 and disclosed in the peer-reviewed literature in 1977.[1]

On the basis of this discovery, Mobil developed the methanol-to-gasoline (MTG) process and ran it commercially in New Zealand for several years. High aromatic contents are no longer environmentally desirable in gasoline; however, methanol catalysis remained an important research topic, and many patents have been issued for the more selective conversion of methanol to light olefins. Methanol-to-olefin (MTO) catalysis, a close relative of MTG chemistry, may be commercialized to meet the increasing demand for polyolefins. Methanol is made from methane in two steps: first it is converted to CO and H_2, and this is then reacted on $Cu/ZnO/Al_2O_3$ or similar catalysts. Thus, the smallest hydrocarbon would be converted to the largest.

Mechanistic investigations of methanol conversion catalysis began immediately.[2,3] It is convenient to treat the overall chemistry as involving five stages for which variable consensus have been reached in the literature. First and quite simply, there is equilibration among methanol, dimethyl ether, and water. Second, on freshly activated catalyst beds, there is often a kinetic induction period that precedes a high yield of hydrocarbon products formed from methanol and dimethyl ether. The third and truly central step is the formation of the first hydrocarbon product. The most important questions in methanol catalysis have been, “What species has the first carbon−carbon bond?” and “How does that bond form?” According to one review,[3] there have been at least 20 distinct mechanisms proposed for methanol catalysis, and higher counts result if subdivisions within broader classes are enumerated. We will discuss this step a little later.

Secondary Reactions: Acid Strength and Catalyst Topology

The fourth stage of methanol conversion catalysis is comprised of secondary reactions that convert the primary olefin product(s) to a mixture of other hydrocarbons. On some materials, notably HZSM-5, secondary reactions consume and mask the primary products. The nature and extent of the reactions of olefins on a microporous solid acid are governed by acid strength, acid site density, catalyst topology, crystallite size, temperature, space velocity, and other process conditions. It is instructive to focus on acid strength and catalyst topology. Figure 1 shows partial structures for three methanol conversion

---

James F. Haw is the Ray Irani CEO of Occidental Petroleum Professor of Chemistry at the University of Southern California. His recognitions include the George A. Olah Award in Hydrocarbon Chemistry of the American Chemical Society and the Yarwood Medal of the British Vacuum Council. He has published over 150 papers, most of them in the areas of catalysis and zeolite chemistry.

Weiguo Song received his Ph.D. from the University of Southern California and continues to work there as a postdoctoral fellow.

David M. Marcus received his B.S. from the University of Miami and is working toward his Ph.D. at the University of Southern California.

John M. Nicholas received his Ph.D. from the University of Illinois−Chicago. He is well-known for his work applying computational chemistry in tightly integrated collaborations with experimental groups. Currently he is a Scientist at Genentech in San Francisco.

10.1021/ar020006o CCC: $25.00

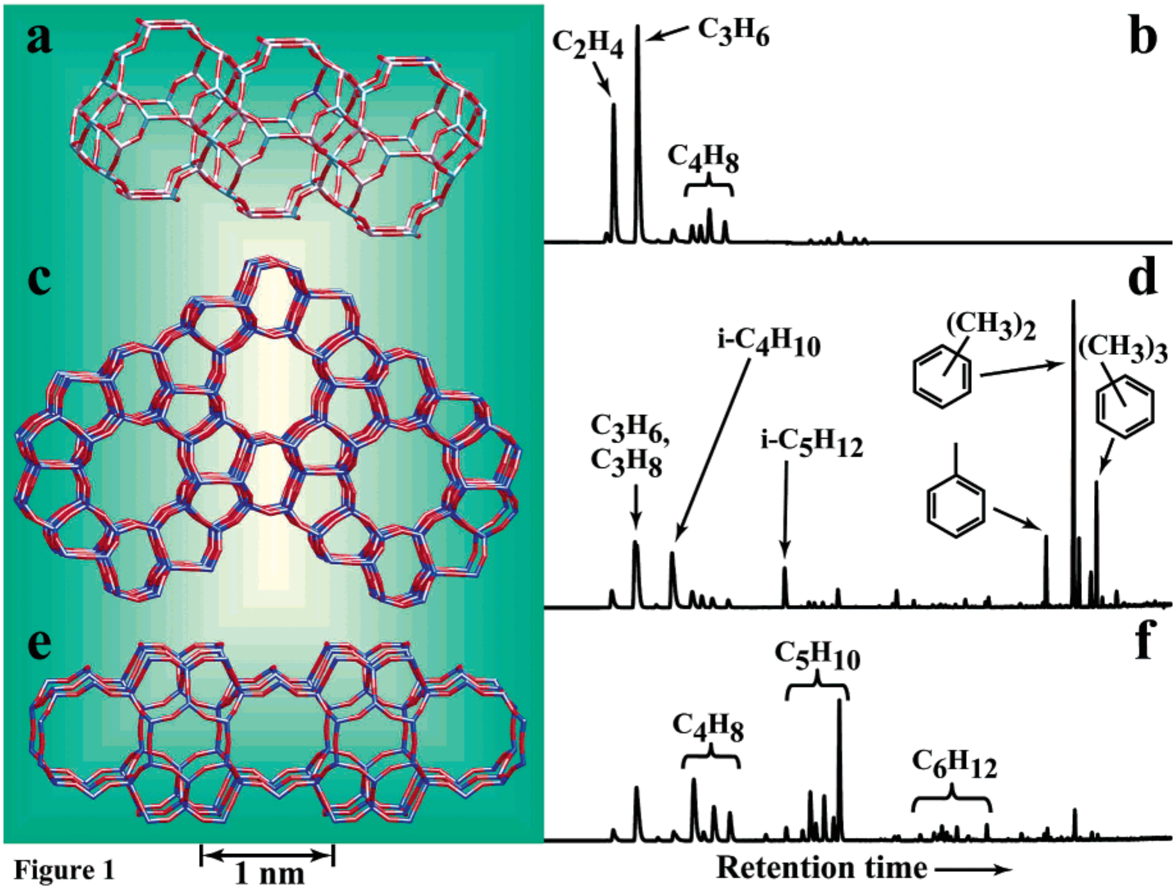

FIGURE 1. Three of the methanol conversion catalysts discussed in this contribution and GC-MS total ion chromatograms illustrating product selectivity on these materials: (a) The CHA topology of the silico-aluminophosphate catalyst HSAPO-34. (b) The products of methanol conversion on HSAPO-34. (c) The MFI structure of the aluminosilicate zeolite HZSM-5. (d) The products of methanol conversion on HZSM-5. (e) The FER topology of H-Ferrierite. (f) The products of methanol conversion on MTO catalysis on H-Ferrierite. Each experiment used 300 mg of catalyst operated at 723 K, and products were sampled 1.5 s following pulsed introduction of 10.2 μL of methanol.

Scheme 1. Olefin Chain-Growth and Cracking Reactions

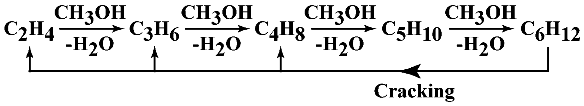

$$C_2H_4 \xrightarrow[-H_2O]{CH_3OH} C_3H_6 \xrightarrow[-H_2O]{CH_3OH} C_4H_8 \xrightarrow[-H_2O]{CH_3OH} C_5H_{10} \xrightarrow[-H_2O]{CH_3OH} C_6H_{12}$$

catalysts and the corresponding chromatograms of the products obtained from methanol on these catalysts at 723 K. The silico-aluminophosphate catalyst HSAPO-34 (Figure 1a) has the chabazite (CHA) structure that features cages ca. 1 nm in dimension that are interconnected through windows that are much smaller, ca. 0.38 nm. These cages form a three-dimensional network structure. Some fairly large molecules can fit in the cages of HSAPO-34, but they cannot migrate from cage to cage; not even benzene can diffuse through the windows connecting cages. Figure 1b shows that the volatile products of methanol conversion on this catalyst are ethylene, propene, smaller amounts of butanes, and traces of linear alkanes. The olefin chain growth process in Scheme 1 does not occur on HSAPO-34, and olefin oligomerization is much less important than it is on the more strongly acidic HZSM-5.

Figure 1c shows a view down one of the two sets of intersecting channels in the aluminosilicate zeolite HZSM-5 (MFI topology). The two-dimensional channel structure of HZSM-5 is based on 10-atom rings versus the eight-atom rings in HSAPO-34, and the channels are wide enough that the C_{2v} isomer of tetramethylbenzene (durene) can diffuse out of the former catalyst. Figure 1d shows that there is little apparent similarity between the products on HZSM-5 and HSAPO-34 (Figure 1b). The HZSM-5 catalyst used in the example produced very little olefin; instead it gave methylbenzenes and light alkanes, especially isobutane and isopentane. The channel intersections of HZSM-5 provide enough volume for cyclization reactions and intermolecular hydride transfer reactions by which a mixture of olefins can be converted into alkanes and aromatics.

The aluminosilicate zeolite H-Ferrierite (FER topology, Figure 1e) has an acid strength very similar to that of HZSM-5, but topological differences result in profoundly different product distributions. The ferrierite catalyst produces almost entirely olefins, especially butenes and pentenes (Figure 1f). The topology of ferrierite is illustrated schematically in Figure 1e; the structure features 10-ring channels running in one direction that are bridged by cages (ferrierite cages) in a second direction. For a molecule to diffuse between a channel and a cage, it must pass through an eight-ring window approximately the

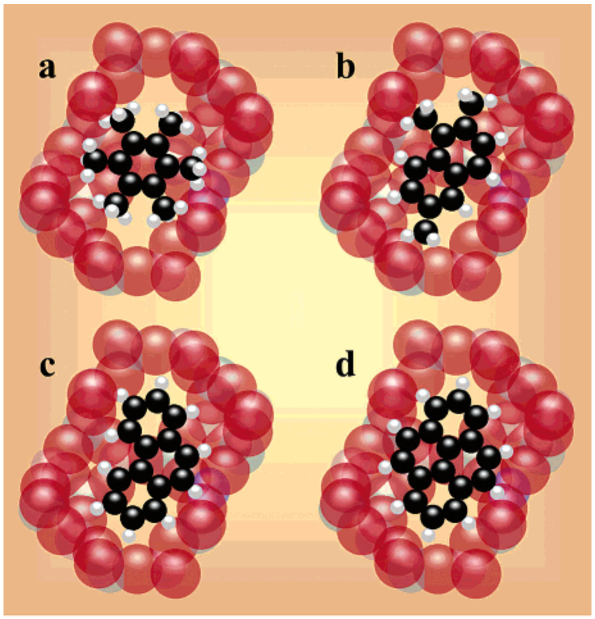

FIGURE 2. Molecular view of MTO catalyst deactivation shown for the specific case of HSAPO-34. (a) Hexamethylbenzene and other methylbenzenes are present in a few percent of cages in an active MTO catalyst. (b) With increasing time on stream, some of the methylbenzenes age into methylnaphthalenes. (c) Further aging to pheananthrene causes a loss of MTO activity in HSAPO-34. (d) The largest ring system to form in HSAPO-34 is pyrene.

same size as that linking the cages in HSAPO-34. There are two principal differences between the ZSM-5 and ferrierite structures: 10-ring channels run in two dimensions in ZSM-5, and their diameters are approximately 10% greater than the one set of 10-ring channels in ferrierite. There is insufficient room in the ferrierite channels for cyclization and intramolecular hydride transfer reactions to occur at appreciable rates. Olefin chain growth (Scheme 1) occurs to the point (hexenes) at which monomolecular cracking becomes efficient, and the olefin distribution tops off at C_5. Methylbenzenes can form in the ferrierite cages, but they cannot pass into the channels and exit the catalyst.

Catalyst Deactivation

The fifth and final stage of methanol conversion in our formalism is catalyst deactivation. We consider the specific case of HSAPO-34, where the process is partly understood as shown schematically in Figure 2. With time on stream, methylbenzenes (Figure 2a) are converted to methylnaphthalenes (Figure 2b).[4] Further aging forms phenanthrene derivatives (Figure 2c), and then pyrene (Figure 2d), the largest aromatic ring system that can be accommodated in the nanocages of this catalyst.[5] Mass transport of reactants and products is greatly reduced once a significant fraction of the cages of HSAPO-34 are occupied by polycyclic aromatics, and the conversion of methanol to volatile products plummets. In industrial use, spent catalyst is regenerated by heating it in air to combust the trapped organic compounds and remove any graphitic carbon deposits from the exterior of catalyst particles.

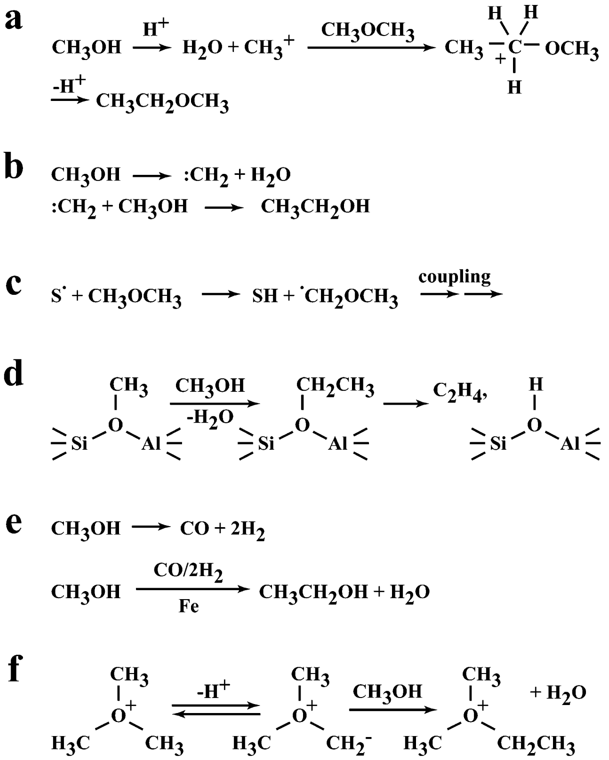

FIGURE 3. Several of the classical "direct" mechanisms for the conversion of methanol/dimethyl ether to olefins (or a direct precursor) shown in highly abbreviated or conflated form: (a) A pathway showing a carbenium ion alkylating dimethyl ether to form a carbonium ion. (b) One of several proposed carbene pathways. (c) An abbreviation of one of several free radical routes. S• is an unspecified surface radical species. (d) An alkoxy chain growth process occurring on a framework site. (e) One of the proposed mechanisms featuring CO, showing a role for transition-metal impurities. (f) An abbreviated oxonium−ylide route.

The Central Mechanistic Problem: The First C−C Bond

Figure 1b suggests that the primary products of methanol conversion on HSAPO-34, the weaker acid, are ethylene, propene, and smaller amounts of butenes. The formation of these primary products has been the central focus of MTO mechanistic studies for many years. Most MTO mechanisms are named after a distinctive intermediate. We already mentioned that that the first proposal envisioned that methanol might be activated on the catalyst to form a carbenium ion, CH_3^+, or carbene, $:CH_2$. Several variations of these mechanisms appeared in the literature, and one of each is outlined in Figure 3a,b. The figure also summarizes examples of some of the other proposed mechanisms for the direct conversion of methanol to a species with a 'first" carbon−carbon bond. Several free radical routes (e.g., Figure 3c) were proposed early on. Methanol can react with zeolite acid sites to form framework bound methoxy (methoxonium) species,[6,7] but the alkoxy chain growth process in Figure 3d has never been observed.

In the Fischer−Tropsch process, CO and H_2 are reacted on iron or other transition metal based catalysts to make linear alkanes. Small amounts of CO are observed in the products streams from MTO and MTG reactors, and iron is an impurity in many catalysts (Figure 3e). In one set of proposed mechanisms, CO was considered to be either an intermediate or a cocatalyst in methanol conversion. In situ NMR studies showed that the reaction rate was invariant with respect to added CO, and when ^{13}CO was added to reacting $^{12}CH_3OH$, no ^{13}C was incorporated in the hydrocarbon products.[8]

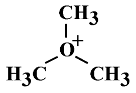

1

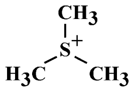

2

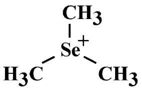

3

One of the difficulties with oxnium-ylide routes (Figure 3f) is deprotonation of the trimethoxonium cation **1**, which should be difficult on an acidic catalyst. In 1991 we used NMR to study the chemistry of dimethyl ether in zeolite HZSM-5; we found that the trimethyl oxonium cation did indeed form (at very high loadings), but it reverted to starting material as the temperature was raised.[9] We also formed trimethylsulfonium **2** and trimethylselenonium **3** cations in the catalyst from the appropriate dimethyl chalcoginides but their presence in no way accelerated the MTO reaction.[10]

The Hydrocarbon Pool

None of the above direct mechanisms explain the observed kinetic induction period. Some workers clearly understood this difficulty and believed that a relatively inefficient direct mechanism functioned only as an "induction reaction" which was followed by more efficient autocatalysis through olefin chain growth (Scheme 1) and cracking.[11] One test of any direct mechanism, either as an induction reaction or the major route on a working catalyst, must be to explain initial primary product selectivity. Most of the proposed direct routes strongly favor ethylene as the primary product, but MTO on HSAPO-34 typically produces more propene than ethylene, even very early in the induction period.

The essential feature of hydrocarbon pool routes is that methanol reacts with entrained hydrocarbon species in the catalyst to begin a sequence of steps leading to primary olefinic products and regeneration of the original hydrocarbon in a catalytic cycle. Figure 4 summarizes several hydrocarbon pool ideas. In 1982 independent papers by Mole and co-workers[12] and Langner[13] appeared that, in retrospect, are so insightful that they could have led to a swift resolution of the MTO mechanism. Mole observed a "cocatalytic" effect when he co-fed toluene with methanol on zeolite HZSM-5, and he proposed a mechanism (shown in Figure 4a) that is similar to the one we favor today. Langner studied the influence of small amounts of higher alcohols on the duration of the induction period.[13] He found an 18-fold reduction in the induction period when the feed contained 3.6 × 10^{-3} mol % cyclohexanol. Langner knew that additional cyloolefins would form from propene under MTO reaction conditions. Finally, he speculated that in methanol conversion catalysis the first olefins formed from impurities in the methanol feed.

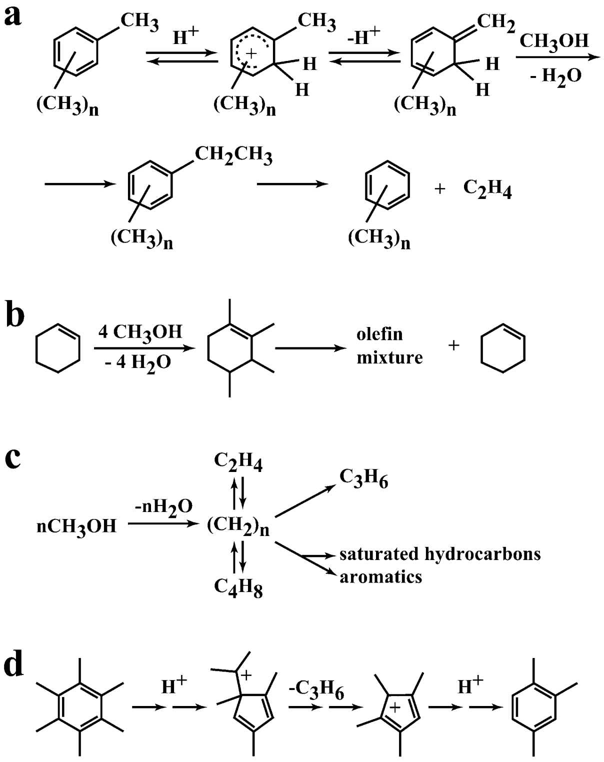

FIGURE 4. Early proposals that have significantly shaped current thinking about the hydrocarbon pool mechanism in MTO catalysis. (a) Mole's 1983 mechanism of methylbenzene side-chain alkylation. (b) An abbreviated account of Langner's explanation for the dramatic effect of cyclohexanol and other co-feeds of reducing the kinetic induction period. (c) Kolboe's early phenomenological hydrocarbon pool mechanism for MTO catalysis. (d) The paring reaction in highly abbreviated form.

Kolboe's contributions to MTO research began in the mid-80's,[14] and in the period of 1993−1996, he proposed that methanol reacted on a hydrocarbon pool of intermediates to form olefins.[15−17] As shown in Figure 4c, Kolboe's original model was schematic, but it had a greater immediate influence that the earlier work of Mole and Langner, and Kolboe continues to make important contributions.[18−20]

A 1961 paper by Sullivan and co-workers[21] on the "paring reaction" has also contributed to recent thinking about the MTO reaction mechanism. The essential feature of the reaction, ring contraction followed by expansion, provides the means to extend an alkyl chain and hence eliminate an olefin from a methylbenzene. Reaction of the aromatic product by methanol or dimethyl ether under MTO conditions would regenerate the original methylbenzene, completing a catalytic cycle.

Identifying the Hydrocarbon Pool

In 1998 we developed a new in situ NMR experiment based on a true flow reactor.[22,23] Figure 5 shows a flow

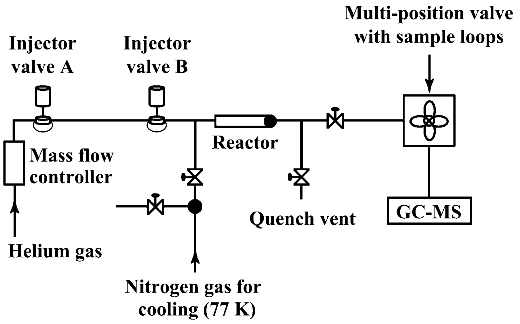

FIGURE 5. Diagram of a pulse-quench catalytic reactor used for mechanistic studies of MTO catalysis. One or more injector valves (two shown) or a syringe pump and a valve are used to treat a catalyst bed in order to prepare some transient state.

reactor with a number of computer-controlled valves for pulsing reagents onto the catalyst bed, collecting product gas samples for GC-MS analysis, and for rapid thermal quenching of the catalyst bed. NMR measurements are made on catalyst beds quenched after the introduction of one or several reagent pulses. The series of ^{13}C MAS NMR spectra in Figure 6 provides a simple but powerful example of the pulse-quench mode of the reactor that is also highly relevant to methanol conversion catalysis.[24] For each result in the figure, a fresh bed of HZSM-5 catalyst was activated at 623 K in a He flow. A pulse of ethylene-$^{13}C_2$ was delivered to the catalyst, and its temperature was rapidly quenched after 0.5−16 s of reaction. Each sample was then analyzed by NMR at room temperature. At short reaction times most of the organic matter retained on the catalyst bed was the 1,3-dimethylcyclopentenyl carbenium ion **4**. After several seconds of reaction, it is apparent that this cation is a precursor to the formation toluene. Thus, this experiment revealed an important part of the mechanism by which methylbenzenes form from olefins on methanol conversion catalysts.


4

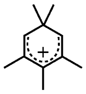
5

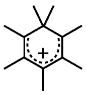
6

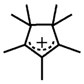
7

In NMR quench reactor studies we published in 1998, we reported evidence strongly supporting a hydrocarbon pool route on HZSM-5; we observed both cation **4**[23] and a second cyclic carbenium ion, the 1,2,2,3,5-pentamethylbenzenium cation **5**[25] from quenched catalyst beds prepared using various methanol conversion conditions. We visualized these cations and closely related neutral species functioning in hydrocarbon pool routes analogous to the Sullivan,[21] Mole,[12] or Langner[13] mechanisms. In a dozen years of using NMR to study carbenium ion chemistry in zeolites we have observed only cyclic, resonance-stabilized tertiary cations to persist on these catalysts, and we developed a theoretical explanation for these observations.[26,27]

We also found ways in which catalyst topology and acid strength could control substitution patterns on persistent carbenium ions that might function as hydrocarbon pool species. Whereas the pentamethylbenzenium cation **5** formed in the channel intersections of medium pore HZSM-5, we readily formed the heptamethylbenzenium cation **6** in the large pore aluminosilicate zeolite H-Beta (BEA topology).[28] We repeatedly failed to synthesize cations **4** or **5** in HSAPO-34, but using a devious route we were able to form the heptamethylcyclopenentyl carbenium ion **7** in the cages of this silicoaluminophosphate.[29] We believe that HSAPO-34 is too weakly acidic to prevent cation **4** from losing a proton (if it formed at all), but deprotonation of cation **7** could occur only by formation of a less favorable exocyclic double bond.

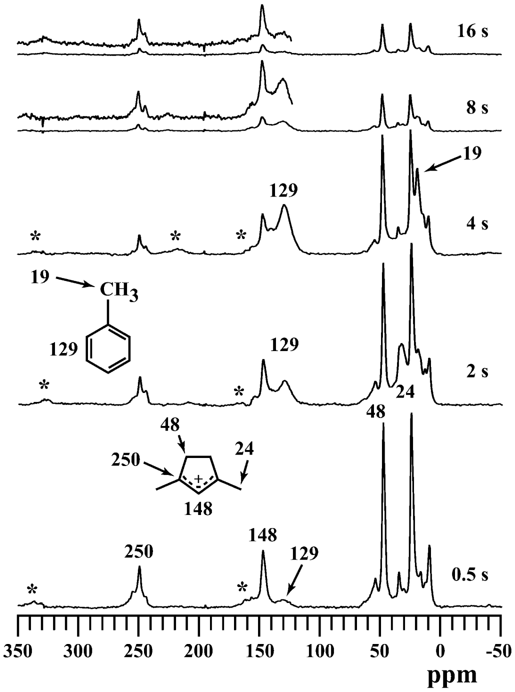

FIGURE 6. ^{13}C CP/MAS solid-state NMR spectra of the reaction products of ethylene-$^{13}C_2$ forming at 623 K on zeolite HZSM-5 catalysts beds. Samples were prepared using the catalytic flow reactor in the previous figure and reaction times of 0.5−16 s.

HZSM-5 catalyst beds with no entrained organic matter showed induction periods before the onset of MTO catalysis, while those with some of the acid sites exchanged with cation **4** were immediately active for the conversion of methanol or dimethyl ether to olefins. Furthermore, if cation **4** was synthesized using ^{13}C-labeled precursors and the reactivity of the catalyst was then probed using methanol-^{12}C, the olefinic products contained a mixture of isotopes. We considered the possibility that cation **4** could transfer a proton back to the zeolite, forming one or more neutral diene isomers that would be readily methylated under MTO conditions. Using theoretical calculations with cluster models of the zeolite, we found several stable states that could be optimized from the components of **4** and an acid site; the two lowest-energy species are shown in Figure 7. At the B3LYP/6-311G** level of theory, the ion pair complex between **4** and the zeolite anion site Z^- was lowest in energy (Figure 7a). Note that one of the protons on **4** is clearly hydrogen bonded to the zeolite cluster. In the neutral π complex

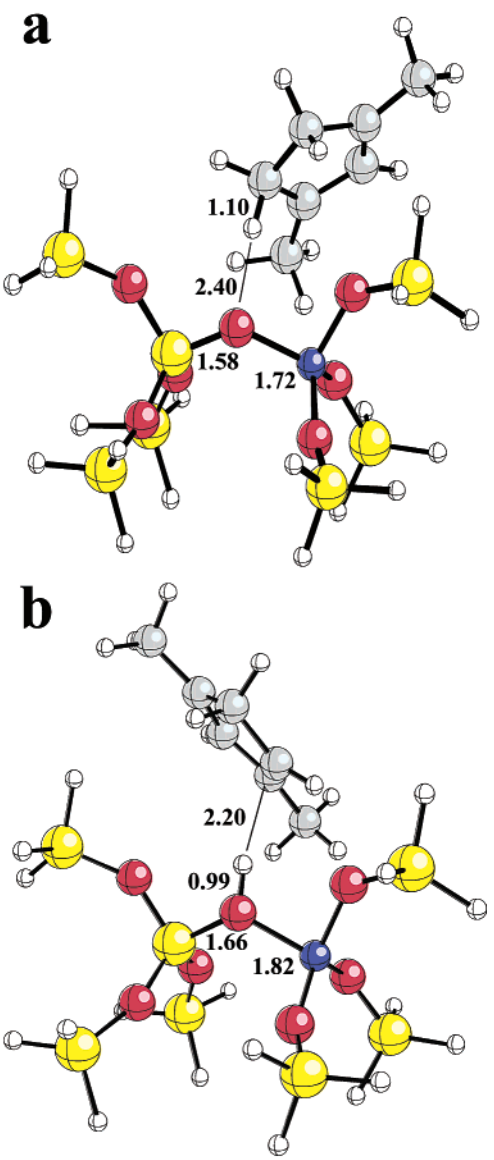

FIGURE 7. B3LYP/6-311G** optimized geometries of species on a cluster model of the acid site of HZSM-5: (a) Ion-pair complex of the 1,3-dimethylyclopentadienyl cation **4** coordinated to the zeolite anion (ion-pair structure). (b) The π complex formed by the neutral cyclic diene and the zeolite acid site.

shown in Figure 7b, this proton has transferred back to the zeolite, and it is hydrogen bonded to one of the double bonds of the cyclic diene. Remarkably, the π complex was only 2.2 kcal/mol higher in energy than the ion pair complex. Of course a reasonably flat potential energy surface, with all intermediates having similar energies and modest barriers connecting these intermediates, is exactly what one should expect for an efficient catalytic pathway.

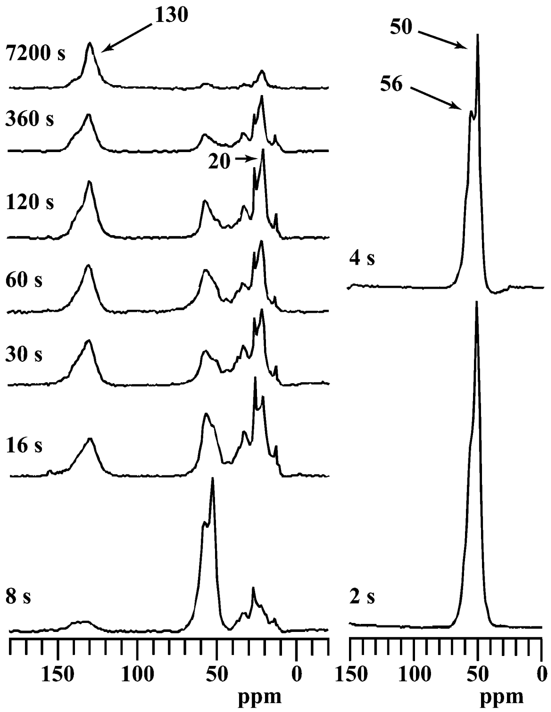

FIGURE 8. ^{13}C CP/MAS NMR spectra of samples from a pulse-quench study of methanol conversion on HSAPO-34 at 673 K. Each sample was prepared by injecting 20 μL of methanol-^{13}C onto a freshly activated catalyst bed (0.3 g) while He was flowed at 600 mLmin^{-1}, and reaction occurred for the times shown followed by a rapid thermal quench.

Silico-aluminophosphate catalysts, especially HSAPO-34 and the topologically very similar HSAPO-18, have been intensely studied in the last several years, in part because secondary reactions are greatly muted on these less acidic catalysts and most of the molecules exiting the catalyst bed are primary MTO products. Because of the lower acidity, cations similar to **4** through **7** are usually not persistent in silico-aluminophosphates; nevertheless we believe that the MTO mechanism is similar to that on the more strongly acidic zeolites, albeit with neutral cyclic species more stable on the former materials. Figure 8 shows ^{13}C spectra from a pulse-quench NMR study of methanol-^{13}C conversion on HSAPO-34 beds at 673 K.[30] At short reaction times, the spectra show unreacted methanol and framework bound methoxy groups (as depicted in the first structure in Figure 3d) at 56 ppm. The yield of olefinic products is very low 4 s after the methanol pulse; the catalyst bed is in the kinetic induction period at this point. After several seconds the aromatic (ca. 130 ppm) and methyl group (20 ppm) signals of methylbenzenes are clearly evident. Over the course of many minutes at reaction temperature, the methyl group signals drop in intensity, but the total aromatic intensity remains constant, as even benzene is unable to pass through the windows connecting the cages in HSAPO-34. GC analysis confirms that as the methyl group signal decreases, olefins exit the catalyst. Furthermore, when methylbenzenes are synthesized in the catalyst using a first methanol pulse and then the catalyst bed activity is subsequently probed with a second methanol pulse, there is no kinetic induction period and methanol conversion is 100%. As seen on HZSM-5, when the methanol in the two pulses differs in carbon isotope, the olefin products of the second pulse have mixed isotopes.

An HSAPO-34 catalyst nanocage with specific contents can be thought of as a specific supramolecular complex.[31] For example, a cage of HSAPO-34 with pentamethylbenzene is one supramolecule $\{Ph(CH_3)_5\}$ and a cage with the same hydrocarbon and two water molecules $\{Ph(CH_3)_5, 2H_2O\}$, is a slightly different supramolecule. A major objective in MTO catalysis is to better control selectivity for ethylene versus propene and higher olefins. We can think of this problem in terms of the relative rate constants for the reactions of each supramolecule to form various olefins. For example, we have $\{Ph(CH_3)_n\} \rightarrow \{Ph(CH_3)_{n-2}, e\}$, where e denotes ethylene, with a rate constant k_n^e, and $\{Ph(CH_3)_n\} \rightarrow \{Ph(CH_3)_{n-3}, p\}$, where p denotes propene, with a rate constant k_n^p. It has been established that the ratio k_n^e/k_n^p decreases with increasing n and increases when water is co-fed with methanol.[31] The water effect can be rationalized in various ways including a reduction in free volume within the supramolecular complex or solvation. The relative activities of various supramolecules must also be considered. Trimethylbenzenes are more selective for ethylene, but hexamethylbenzene (which favors propene) is far more active.

There are in principle a number of ways to vary the structure of the supramolecular complex. First, as the catalyst ages the methylbenzenes are replaced by larger aromatic compounds, notably methylnaphthalenes. As an HSAPO-34 catalyst bed approaches deactivation, ethylene selectivity increases (albeit with a decrease in total olefin yield). This suggested the possibility that supramolecules with methylnaphthalene centers are more selective for ethylene, which we verified by synthesizing these supramolecules selectively.[32] As another example, we found conditions under which we could partially oxidize methylbenzenes in HSAPO-34 to methylphenols $\{Ph(CH_3)_nOH\}$ and found that we could easily methylate these species up to $n = 5$. Unfortunately these complexes showed no MTO activity whatsoever.[33] While it is true that $-OH$ (and $-OCH_3$) groups tend to activate aromatic rings for alkylation and dealkylation reactions, they are also very basic functional groups (in the gas phase). Thus, the wrong part of the molecule is almost certainly protonated or methylated. We also used a ship-in-a-bottle strategy to introduce inorganic species into the nanocages of HSAPO-34. By cofeeding methanol and PH_3 (a highly toxic, pyrophoric gas), we assembled $P(CH_3)_4^+$ cations in most or all cages, depending on the conditions used. As expected, this material is not an active MTO catalyst, but calcination in air burns out the carbon leaving a poorly characterized phosphate species with a broad ^{31}P NMR signal. This modified material is an active catalyst with improved ethylene selectivity.[34]

While the evidence for some kind of hydrocarbon pool mechanism in methanol conversion catalysis is considerable, much remains to be discovered about the details of how the hydrocarbon pool functions. Side-chain alkylation (as first described by Mole) and the paring mechanism (originally described by Sullivan) are competing detailed mechanisms for the hydrocarbon pool. Large pore catalysts such as HBeta or HSAPO-5 (AFI topology) can be used to study the reactions of compounds or mixtures that would be less conveniently synthesized in, for example, HSAPO-34. Figure 9 shows GC-MS total-ion chromatograms of products from a series of experiments in which methylbenzenes were pulsed onto HBeta catalyst beds at 723 K.[35] 1,2,4,5-Tetramethylbenzene alone (Figure 9a) disproportionates to a mixture of methylbenzenes but produces only a trace of olefin product; however, as shown in Figure 9b, the olefin yield from a pulse of hexamethylbenzene is higher. Figure 9c shows that co-injection of toluene with a 5-fold molar excess of methanol-^{13}C produced far a far greater yield of olefin products than was obtained with hexamethylbenzene alone. As a control experiment, we also studied hexamethylbenzene and water (5:1 mol:mol). In this case (Figure 9d) the yield of olefins was very modest, similar to hexamethylbenzene alone (Figure 9b) rather than toluene and methanol (Figure 9c). If paring were the dominant route from methanol to olefins and the reaction of methanol with toluene to form hexamethylbenzene went to completion before olefin formation, then the experiments in Figure 9c,d should have involved the same reactants (hexamethylbenzene and water). Because a mixture of toluene and 5 equiv of methanol is far more active than hexamethylbenzene and water, we believe that a side-chain route is more important than paring under these conditions.

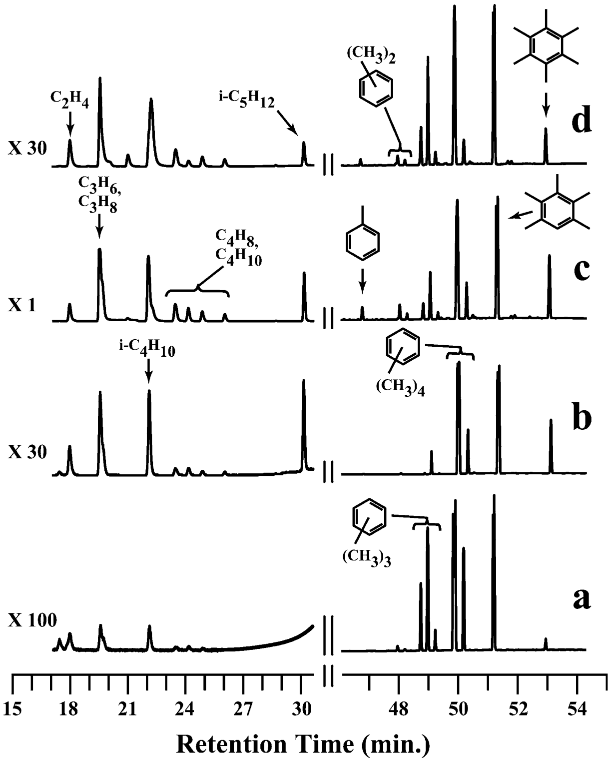

FIGURE 9. GC-MS total ion chromatograms from experiments probing the reactions of methylbenzenes either alone or with methanol-^{13}C. All experiments shown were carried out at 723 K using HBeta with $SiO_2/Al_2O_3 = 75$ and gas sampling at 1.5 s. (a) Durene alone, showing a very low yield of olefins. (b) Hexamethylbenzene alone showing a modest yield of olefins. (c) Methanol-^{13}C and toluene 5:1 (mol:mol) produced the highest yield of olefins. (d) Control experiment using water and hexamethylbenzene 5:1 (mol:mol).

The paring mechanism predicts that carbon labels from methanol will find their way into aromatic ring positions and labeled carbons originally in the rings will also end up in olefin products. Such scrambling does occur and

Scheme 2. A Detailed Side-Chain Route to Propene Based on Deprotonation of Cation 6

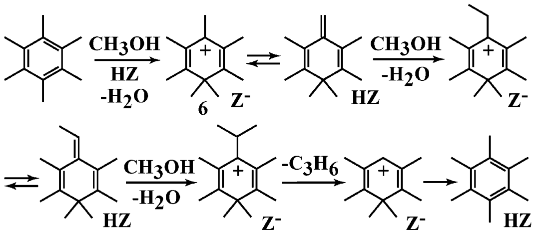

aromatic carbon ring scrambling seems to correlate with hydrocarbon pool catalytic activity; for example, it occurs more rapidly on hexamethylbenzene than on toluene, and not at all on inactive species such as methylphenols or pyrene in HSAPO-34. However, scrambling of aromatic ring carbons could also occur through other mechanisms such as tropylium ion routes, i.e., 6 to 7 to 6. Paring probably contributes to MTO activity, at least under some conditions, but more study of ring label scrambling is needed before its contribution can be quantified.

In situ NMR clearly shows the formation of the heptamethylbenzenium cation **6** on zeolite HBeta. Scheme 2 shows how this cation would transfer a proton back to the zeolite conjugate base (Z^-) to form an exo-cyclic olefin which then undergoes a series of methylation and deprotonation steps leading to loss of an olefin product and (after remethylation) completion of a catalytic cycle. Theoretical modeling supports the reasonableness of this mechanism[36] but so far cannot rule out the possibility of other routes functioning as well.

Whither the Induction Reaction?

The hydrocarbon pool mechanism predicts that olefin synthesis takes place on larger organic species (which we call organic reaction centers) through a sequence of methylation steps leading to elimination of an olefin and re-initialization of the catalytic cycle. The organic reaction center is a scaffold on which the reactants are tacked together and from which the product is removed. The organic reaction center allows chemistry that might otherwise require exotic, high-energy species to take place by way of cyclic, resonance-stabilized, secondary and tertiary cation intermediates that are structurally related to well characterized species identified by NMR on the actual MTO catalysts.

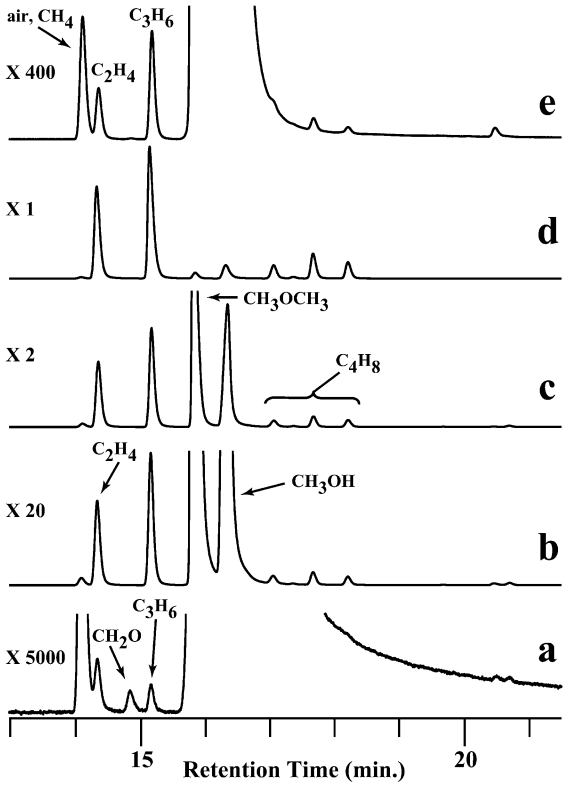

FIGURE 10. GC (FID detector) analyses of the product streams sampled 2.4 s after pulsing 12.5 μL methanol onto 300 mg beds of HSAPO-34 at 648 K. Samples a–d are from a single bed of rigorously calcined HSAPO-34 following a series of pulses of fractionally distilled methanol delivered in 30 min intervals. (a) Following the first pulse, the total yield of volatile hydrocarbons was ca. 26 ppm. (b) Following a second methanol pulse the yield of volatile hydrocarbon products increased to 1.5%. (c) Following a third, methanol pulse the yield further increased to 10%. (d) This catalyst bed was reacted with an additional 200 μL of methanol to create a larger hydrocarbon pool. 30 min later another 12.5 μL methanol pulse gave nearly complete conversion. (e) Following the first pulse of fractionally distilled methanol onto a fresh HSAPO-34 bed prepared using the standard calcination procedure but not the more rigorous second calcination. The volatile hydrocarbon yield, 590 ppm, was substantially higher without rigorous calcination, cf. (a).

On a working catalyst, reaction centers convert methanol to olefins, and some of the olefins make additional reaction centers. But where do the first reaction centers come from, and exactly what happens during the kinetic induction period? For example, a direct mechanism might operate very slowly during the induction period until sufficient reaction centers are present for autocatalysis. We set out to study this presumptive reaction, but the closer we looked, the less we saw. In one series of unpublished experiments we found small amounts of ethylene forming with near-100% selectivity during the induction period on HSAPO-34, but we quickly attributed this to a 100 ppm ethanol impurity in the methanol. Other reagent methanol samples contained 2-propanol, propanol, acetone, or acetaldehyde, and these all readily form methylbenzenes on solid acid catalysts. We also found that the catalysts sometimes contained aromatics formed through incomplete calcination of templating agents. Figure 10 shows one set of results from our efforts to reduce the contributions of organic impurities to the initiation of MTO catalysis.[37] We pulsed several shots of methanol containing only ca. 11 ppm total organic impurities onto highly purified HSAPO-34 at 648 K and measured product yields after each successive pulse. The total yield of volatile hydrocarbons after the first pulse was an astonishingly low 0.0026%, but this crept up with successive pulses as a larger hydrocarbon pool was established. Note in Figure 10a that the ethylene/propene selectivity is not obviously different from that obtained on the same catalyst with maturation of the hydrocarbon pool. Most of the direct mechanisms predict the formation of ethylene, and ethylene selectivity is not elevated in Figure 10a. On the basis of the evidence in Figure 10, we see no need to invoke any direct induction mechanism for converting methanol to olefins, at least for temperatures of 648 K or lower. Only a few ppm of organic impurities in the methanol suffice for the creation of a primordial hydrocarbon pool which forms during the induction period and grows with increases in olefin yield. The rate of all possible direct routes for methanol conversion may or may not be exactly zero at higher temperatures or with other conditions, but we have yet to observe any unusual selectivity that we can assign to the operation of a direct mechanism during the induction period.

MTO: A Unifying Problem in Catalysis

The active site for MTO catalysis is not a proton on a rarefied piece of clay. It is an organic–inorganic hybrid that will come to be understood through a fusion of structure–activity and topological concepts. The detailed reactions of the hydrocarbon pool encompass alkylation and isomerization of methylbenzenes, homologation, oligomerization, cracking, and isomerization of olefins, and cyclization and hydride transfer reactions inherent in disproportionation to aromatics and alkanes. Thus, a fuller understanding of MTO catalysis will necessarily benefit other important, fundamental problems in hydrocarbon catalysis on solid acids. MTO hydrocarbon pool mechanisms involve distinct supramolecular species with clearly definable chemical properties. Thus, MTO catalysis will continue to be a very attractive test case for the application and refinement of theoretical modeling and in situ spectroscopy to catalysis. The molecular vocabulary of MTO catalysis invites synergy between homogeneous and heterogeneous catalysis.

This work was supported by the National Science Foundation (CHE-0205939) and the U.S. Department of Energy (DOE) Office of Basic Energy Sciences (BES) (Grant No. DE-FG03-93ER14354).

References

(1) Chang, C. D.; Silvestri, A. J. Conversion of Methanol and other O–Compounds over Zeolite Catalysts. *J. Catal.* **1977**, *47*, 249–259.
(2) Chang, C. D. Hydrocarbons from Methanol. *Catal. Rev.* **1983**, *25*, 1–118.
(3) Stöcker, M. Methanol-to-Hydrocarbons: Catalytic Materials and their Behavior. *Microporous Mesoporous Mater.* **1999**, *29*, 3–48.
(4) Fu, H.; Song, W.; Haw, J. F. Polycyclic Aromatics Formation in HSAPO-34 during Methanol-to-Olefin Catalysis: ex Situ Characterization after Cryogenic Grinding. *Catal. Lett.* **2001**, *76*, 89–94.
(5) Marcus, D. M.; Song, W.; Ng, L. L.; Haw, J. F. Aromatic Hydrocarbon Formation in HSAPO-18 Catalysts: Cage Topology and Acid Site Density. *Langmuir* **2002**, *18*, 8386-8391.
(6) Forester, T. R.; Howe, R. F. In Situ FTIR Studies of Methanol and Dimethyl Ether in HZSM-5. *J. Am. Chem. Soc.* **1987**, *109*, 5076–5082.
(7) Murray, D. K.; Chang, J.-W.; Haw, J. F. Conversion of Methyl Halides to Hydrocarbons on Basic Zeolites: A Discovery by in Situ NMR. *J. Am. Chem. Soc.* **1993**, *115*, 4732–4741.
(8) Munson, E. J.; Lazo, N. D.; Moellenhoff, M. E.; Haw, J. F. CO Is neither an Intermediate nor a Catalyst in MTG Chemistry on Zeolite HZSM-5. *J. Am. Chem. Soc.* **1991**, *113*, 2783–2786.
(9) Munson, E. J.; Haw, J. F. NMR Observation of Trimethyloxonium Formation from Dimethyl Ether on Zeolite HZSM-5. *J. Am. Chem. Soc.* **1991**, *113*, 6303–6305.
(10) Munson, E. J.; Khier, A. A.; Haw, J. F. An in Situ Solid-State Study of the Formation and Reactivity of Trialkylonium Ions in Zeolites. *J. Phys. Chem.* **1993**, *97*, 7321–7327.
(11) Dessau, R. M. On the H-ZSM-5 Catalyzed Formation of Ethylene from Methanol or Higher Olefins. *J. Catal*. **1986**, *99*, 111–116.
(12) Mole, T.; Bett, G.; Seddon, D. Conversion of Methanol to Hydrocarbons over ZSM-5 Zeolite – an Examination of the Role of Aromatic-Hydrocarbons Using Carbon-14-Labeled and Dueterium-Labeled Feeds. *J. Catal*. **1983**, *84*, 435–445.
(13) Langner, B. E. Reactions of Methanol on Zeolites with Different Pore Structures. *Appl. Catal.* **1982**, *2*, 289–302.
(14) Kolboe, S. Methanol Reactions on ZSM-5 and Other Zeolite Catalysts – Autocatalysis and Reaction-Mechanism. *Acta Chem. Scand.* **1986**, *A-40*, 711–713.
(15) Dahl, I. M.; Kolboe, S. On the Reaction-Mechanism for Propene Formation in the MTO Reaction over SAPO-34. *Catal. Lett.* **1993**, *20*, 329–336.
(16) Dahl, I. M.; Kolboe, S. On the Reaction-Mechanism for Hydrocarbon Formation from Methanol over SAPO-34. 1. Isotopic Labeling Studies of the Co–Reaction of Ethene and Methanol. *J. Catal.* **1994**, *149*, 458–464.
(17) Dahl, I. M.; Kolboe, S. On the Reaction Mechanism for Hydrocarbon Formation from Methanol over SAPO-34. 2. Isotopic Labeling Studies of the Co–Reaction of Propene and Methanol. *J. Catal.* **1996**, *161*, 304–309.
(18) Mikkelsen, O.; Ronning, P. O.; Kolboe, S. Use of Isotopic Labeling for Mechanistic Studies of the Methanol-to-Hydrocarbons Reaction. Methylation of Toluene with Methanol over H-ZSM-5, H-Mordenite and H-Beta. *Microporous Mesoporous Mater.* **2000**, *40*, 95–113.
(19) Arstad, B.; Kolboe, S. Methanol-to-Hydrocarbons Reaction over SAPO-34. Molecules Confined in the Catalyst Cavities at short Time on Stream. *Catal. Lett.* **2001**, *71*, 209–212.
(20) Arstad, B.; Kolboe, S. The Reactivity of Molecules Trapped within the SAPO-34 Cavities in the Methanol-to-Hydrocarbons Reaction. *J. Am. Chem. Soc.* **2001**, *123*, 8137–8138.
(21) Sullivan, R. F.; Egan, C. J.; Langlois, G. E.; Sieg, R. P. A New Reaction that Occurs in the Hydrocracking of Certain Aromatic Hydrocarbons. *J. Am. Chem. Soc.* **1961**, *83*, 1156–1160.
(22) Haw, J. F.; Goguen, P. W.; Xu, T.; Skloss, T. W.; Song, W.; Wang, Z. In Situ NMR Investigations of Heterogeneous Catalysis with Samples Prepared under Standard Reaction Conditions. *Angew. Chem.* **1998**, *37*, 948–949.
(23) Goguen, P. W.; Xu, T.; Barich, D. H.; Skloss, T. W.; Song, W.; Wang, Z.; Nicholas, J. B.; Haw, J. F. Pulse-Quench Reactor Studies Reveal a Carbon-Pool Mechanism in Methanol-to-Gasoline Chemistry on Zeolite HZSM-5. *J. Am. Chem. Soc.* **1998**, *120*, 2650–2651.
(24) Haw, J. F.; Nicholas, J. B.; Song, W.; Deng, F.; Wang, Z.; Heneghan, C. S. Roles for Cyclopentenyl Cations in the Synthesis of Hydrocarbons from Methanol on Zeolite Catalyst HZSM-5. *J. Am. Chem. Soc.* **2000**, *122*, 4763–4775.
(25) Xu, T.; Barich, D. H.; Goguen, P. W.; Song, W.; Wang, Z.; Nicholas, J. B.; Haw, J. F. Synthesis of a Benzenium Ion in a Zeolite with Use of a Catalytic Flow Reactor. *J. Am. Chem. Soc.* **1998**, *120*, 4025–4026.
(26) Nicholas, J. B.; Haw, J. F. The Prediction of Persistent Carbenium Ions in Zeolites. *J. Am. Chem. Soc.* **1998**, *120*, 11804–11805.
(27) Song, W.; Nicholas, J. B.; Haw, J. F. Acid–Base Chemistry of a Carbenium Ion in a Zeolite under Equilibrium Conditions: Verification of a Theoretical Explanation of Carbenium Ion Stability. *J. Am. Chem. Soc.* **2001**, *123*, 121–129.
(28) Song, W.; Nicholas, J. B.; Sassi, A.; Haw, J. F. Synthesis of the Heptamethylbenzenium Cation in Zeolite-β: in Situ NMR and Theory. *Catal. Lett.* **2002**, *81*, 49–53.
(29) Song, W.; Nicholas, J. B.; Haw, J. F. A Persistent Carbenium Ion on the Methanol-to-Olefin Catalyst HSAPO-34: Acetone Shows the Way. *J. Phys. Chem. B* **2001**, *105*, 4317–4323.
(30) Song, W.; Haw, J. F.; Nicholas, J. B.; Heneghan, K. Methylbenzenes Are the Organic Reaction Centers for Methanol-to-Olefin Catalysis on HSAPO-34. *J. Am. Chem. Soc.* **2000**, *122*, 10726–10727.
(31) Song, W.; Fu, H.; Haw, J. F. Supramolecular Origins of Product Selectivity for Methanol-to-Olefin Catalysis on HSAPO-34. *J. Am. Chem. Soc.* **2001**, *123*, 4749–4754.
(32) Song, W.; Fu, H.; Haw, J. F. Selective Synthesis of Methylnaphthalenes in HSAPO-34 Cages and Their Function as Reaction Centers in Methanol-to-Olefin Catalysis. *J. Phys. Chem. B* **2001**, *105*, 12839–12843.
(33) Fu, H.; Song, W.; Marcus, D. M.; Haw, J. F. Ship-in-a-Bottle Synthesis of Methylphenols in HSAPO-34 Cages from Methanol and Air. *J. Phys. Chem. B.* **2002**, *106*, 5648–5652.

(34) Song, W.; Haw J. F. Improved Methanol-to-Olefin Catalyst with Nanocages Functionalized through Ship-in-a-Bottle Synthesis from PH_3. *Angew. Chem.* **2003**, *42*, 891−894.

(35) Sassi, A.; Song, W.; Wildman, M. A.; Ahn, H. J.; Prasad, P.; Nicholas, J. B.; Haw, J. F. Methylbenzene Chemistry on Zeolite HBeta: Multiple Insights into Methanol-to-Olefin Catalysis. *J. Phys. Chem. B.* **2002**, *106*, 2294−2303.

(36) Arstad, B.; Nicholas, J. B.; Haw, J. F. Unpublished results, 2003.

(37) Song, W.; Marcus, D. M.; Fu, H.; Ehresmann, J. O.; Haw, J. F. An Oft-Studied Reaction That May Never Have Been: Direct Catalytic Conversion of Methanol or Dimethyl Ether to Hydrocarbons on the Solid Acids HZSM-5 or HSAPO34. *J. Am. Chem. Soc.* **2002**, *124*, 3844−3845.

AR020006O